



Article

# Study of Aluminum Wires Treated with MoB<sub>2</sub> Nanoparticles

David Florián-Algarín <sup>1</sup> , Angelisse Ramos-Morales <sup>1</sup>, Michelle Marrero-García <sup>2</sup> and Oscar Marcelo Suárez <sup>3,\*</sup>

<sup>1</sup> Department of Civil Engineering, University of Puerto Rico-Mayagüez, Mayagüez, PR 00681, USA; david.florian@upr.edu (D.F.-A.); angelisse.ramos@upr.edu (A.R.-M.)

<sup>2</sup> Department of Mechanical Engineering, University of Puerto Rico-Mayagüez, Mayagüez, PR 00681, USA; michelle.marrero5@upr.edu

<sup>3</sup> Department of Engineering Science and Materials, University of Puerto Rico-Mayagüez, Mayagüez, PR 00681, USA

\* Correspondence: oscarmarcelo.suarez@upr.edu; Tel.: +1-787-832-4040 (ext. 5812)

Received: 22 June 2018; Accepted: 18 August 2018; Published: 21 August 2018



**Abstract:** This research focuses on the fabrication of aluminum wires treated with MoB<sub>2</sub> nanoparticles and their effect on selected mechanical and thermal properties of the wires. These nanoparticles were obtained by fragmentation in a high-energy ball mill and then mechanically alloyed with pure aluminum powder to form Al/MoB<sub>2</sub> pellets. The pellets were added to molten pure aluminum (99.5%) at 760 °C. Afterwards, the treated melt was cast into cylindrical ingots, which were cold-formed to the desired final diameter with intermediate annealing. X-ray diffraction and optical microscopy allowed characterizing the structure and microstructure of the material. The wires underwent tensile and bending tests, as well as electrical measurements. Finally, this research demonstrated how the mechanical properties of aluminum wires can be enhanced with the addition of MoB<sub>2</sub> nanoparticles with minimal effects on the material resistivity.

**Keywords:** aluminum wires; MoB<sub>2</sub>; nanoparticles; electrical resistivity

## 1. Introduction

Many challenges regarding low-cost fabrication processes and better properties of electronic packages have compelled researchers to investigate composites made of aluminum/diamond and aluminum/graphene. These materials possess appealing properties, such as low coefficient of thermal expansion (CTE) and high thermal conductivity [1–7]. In that respect, different authors demonstrated how the addition of diamond is beneficial in electronic high power and high temperature applications [4].

More recently, at the University of Puerto Rico—Mayagüez, several projects demonstrated the effectiveness of adding nanoparticles to Al wires to improve their mechanical properties. In particular, through an advanced procedure, these researchers demonstrated how the addition of MgB<sub>2</sub> nanoparticles increased the ultimate tensile strength (UTS) of the said wires with only a small decrease in electrical conductivity [8]. Also, in a comparative study using NbB<sub>2</sub> and ZrB<sub>2</sub> nanoparticles, it was found that while both diborides raised the maximum tensile strength of the wires; in this case, only the wires bearing ZrB<sub>2</sub> nanoparticles did not present significant electrical conductivity losses [9].

Accordingly, the present study focused on the fabrication and characterization of aluminum/MoB<sub>2</sub> composite wires. In particular, the effect of MoB<sub>2</sub> nanoparticles addition on the wires CTE and electrical conductivity was investigated. The ultimate goal has been to evaluate how different levels of MoB<sub>2</sub> can affect the wires strength, electrical response, and the feasibility of spooling the wires without fracturing

via a coiling test. To our knowledge, this is the first report showing advanced characterization of both the electrical and mechanical properties of aluminum wires reinforced with MoB<sub>2</sub> nanoparticles.

## 2. Experimental Procedure

The size of the MoB<sub>2</sub> particles (provided by Alfa Aesar, Ward Haverhill, MA, USA) was reduced by fragmentation in a vario-planetary high-energy ball mill (Pulverisette 4, manufactured by Fritsch GmbH, Idar Oberstein, Germany). The process, which is described in a prior publication [1], was completed in 5 h at 1600 rpm. To track the fragmentation process, we took samples every hour to be analyzed using X-ray diffraction Siemens<sup>®</sup> (Princeton, NJ, USA) D500 diffractometer, with Cu K $\alpha$  radiation ( $\lambda = 0.154178$  nm). Using Scherrer's equation [10], the X-ray diffraction patterns allowed determining the average crystallite size of the milled powders.

Afterwards, by mixing 0.9 g of MoB<sub>2</sub> nanoparticles with 17.1 g of pure Al powder (Acros Organics, Morris Plains, NJ, USA) we prepared a nanocomposite containing 5% nanoparticles embedded in 95% aluminum via ball-milling. These ball-milled nanocomposite pellets were sintered at 260 °C under a reduced atmosphere (roughly 4 kPa). An Epiphot 200 (Nikon<sup>®</sup>, Melville, NY, USA) metallurgical microscope and a Siemens<sup>®</sup> (Princeton, NJ, USA) D500 X-ray diffractometer allowed confirming the pellet fabrication effectiveness as a uniform distribution of MoB<sub>2</sub> particles embedded in an Al matrix.

We added the Al/MoB<sub>2</sub> pellets into a pure aluminum (99.5%) melt held at 760 °C in an electrical furnace furnished with a graphite crucible. The molten metal was stirred to procure a uniform nanoparticles distribution. Thereupon, the crucible content was poured into cylindrical molds to produce 6 mm diameter ingots. To make the wires we cold-rolled the ingots down to 1.4 mm in diameter, i.e., with a cross area reduction of 94.5%. A full annealing (5 h at 400 °C) allowed softening the wires. Thus, we were capable of continuing the cold rolling to produce wires with a 1 mm diameter, i.e., a final cross area reduction of 97.2%. A final cold drawing without area reduction allowed a wire with a more uniform diameter.

The microstructures of the pellets and wires (at different stages of the manufacturing process), were observed in a Nikon<sup>®</sup> (Melville, NY, USA) Epiphot 200 optical microscope. Standard tensile tests at room temperature (25 °C) were conducted in a low-force universal testing machine Instron<sup>®</sup> (Norwood, MA, USA) model 5944, according to ASTM B 230/B 230M-07 [11].

Finally, we measured the wires electrical resistance using a four-point probe technique, developed in a prior research [12]. With the geometry of each sample we computed the electrical conductivity of the material, which was expressed in terms of percent of the International Annealed Copper Standard (IACS) [13].

## 3. Results and Discussion

After the X-ray diffraction (XRD) analysis, the ensuing Al/MoB<sub>2</sub> nanocomposite pellets were added to the said molten aluminum. The cylindrical ingots cast, as mentioned, allowed fabricating the wires, which were later characterized using a coiling test, and via tensile and electrical conductivity experiments. The following section details these results.

### 3.1. Study of the Nanoparticles and Nanocomposite Pellets

We determined the most time-efficient milling procedure to produce the MoB<sub>2</sub> nanoparticles at 1600 rpm using XRD of the powders milled upon several times: 1 to 5 h. Figure 1 shows the diffractograms of the ball-milled MoB<sub>2</sub> specimens as a function of the milling time. As mentioned, Scherrer's equation permitted to estimate the average size of the ball milled diboride, based on the width of a characteristic peak. For the remaining of research stage, we used particles with five milling hours since, according to Figure 2, this time presented the smallest size dispersion. The error bars (obtained via a statistical t-distribution with 0.95% confidence level) indicate a small data dispersion at four milling hours. We believe that shorter and longer times could result in non-uniform sizes and cluster agglomerations, respectively.

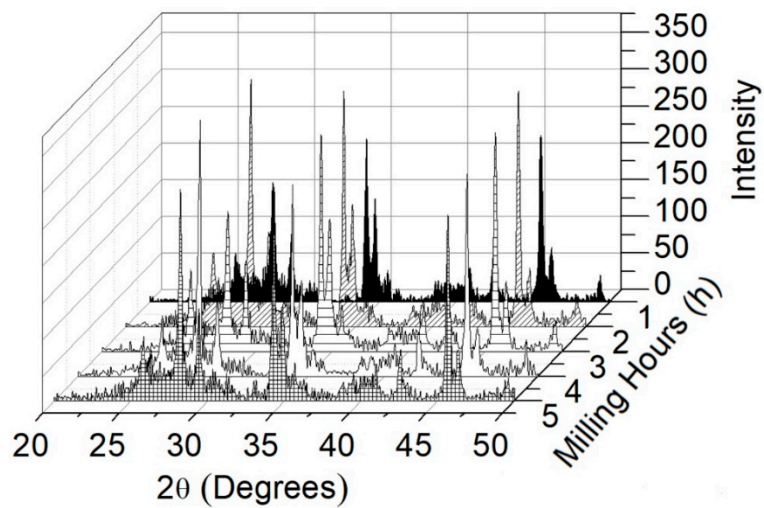


Figure 1. X-ray diffraction (XRD) patterns of MoB<sub>2</sub> specimens at different milling hours.

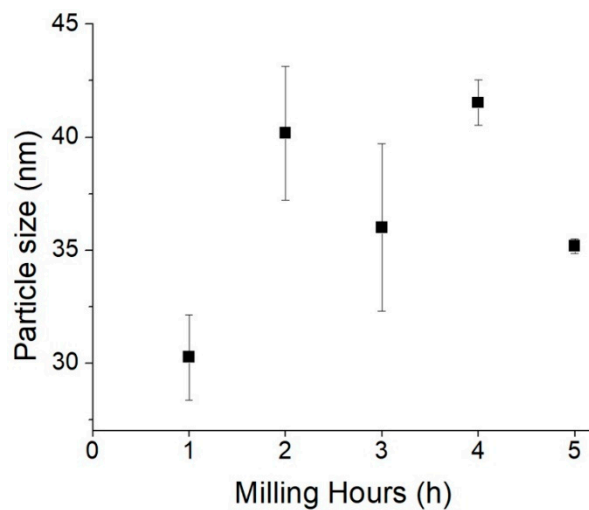


Figure 2. Average MoB<sub>2</sub> particle size vs. time of high-energy ball milling.

### 3.2. Nanocomposite Pellets

Thereupon, the MoB<sub>2</sub> nanoparticles were mixed with Al powder (99.9% purity) and milled for one hour to make the pellets using the same vario-planetary system. The ball milling parameters and procedure were optimized in prior research [14].

To enhance the Al/MoB<sub>2</sub> interface, the pellets were sintered in a reduced vacuum atmosphere at 260 °C for ½ h. Optical micrographs (Figure 3) allowed corroborating that the MoB<sub>2</sub> particles were well-distributed and embedded into the Al matrix. X-ray diffraction permitted verification that no unexpected phase (e.g., oxides) formed upon processing (Figure 4).



**Figure 3.** Optical micrographs of the Al/MoB<sub>2</sub> nanocomposite pellets: (A) at low magnification; (B) at higher magnification.

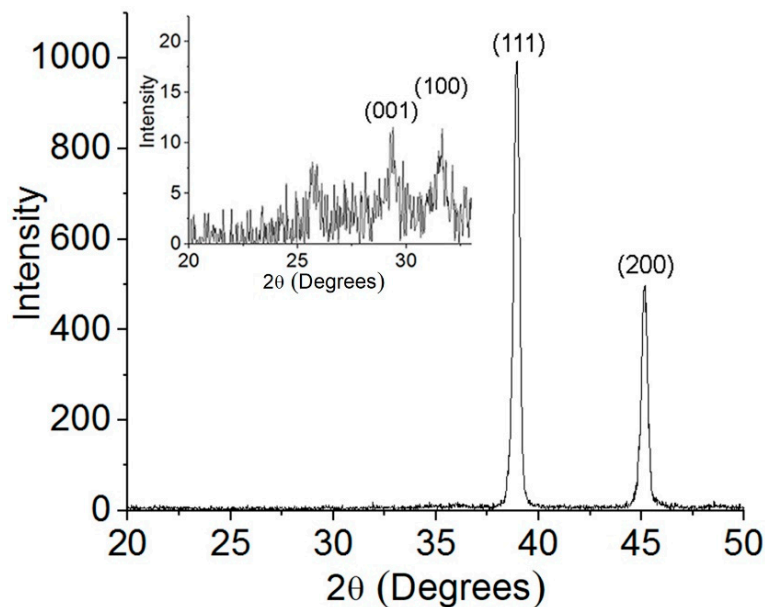


**Figure 4.** XRD pattern of Al/MoB<sub>2</sub> composite pellet after sintering. The inset displays a close-up indicating reflections from the MoB<sub>2</sub> crystallographic planes [15].

### 3.3. Wires Coiling Test

The coiling test of the wires followed the ASTM B230/B230M standard; this regulates how to loop the wire around a rod with identical diameter [11]. Hence, those tests reveal whether it is feasible to form a spool with wires without breaking or cracking them. As Figures 5–8 demonstrate, most aluminum wires either untreated or treated with MoB<sub>2</sub> did not display any crack. The only wire that showed some apparent fissures was the one bearing 1% MoB<sub>2</sub> (Figure 9). For this reason, we did not continue characterizing this wire as it did not comply with the aluminum standard 1350-H19 [11].

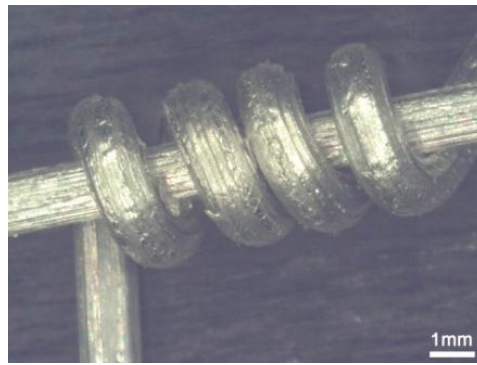


**Figure 5.** Pure Al wire used for reference.

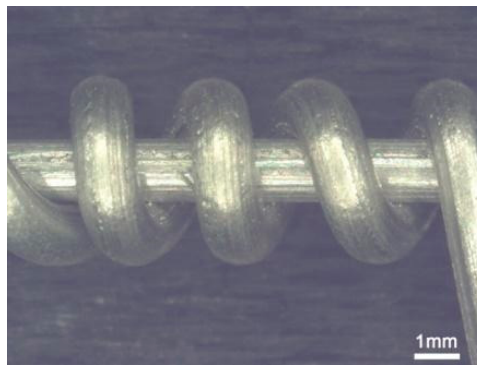


**Figure 6.** 0.25 wt.% MoB<sub>2</sub>.

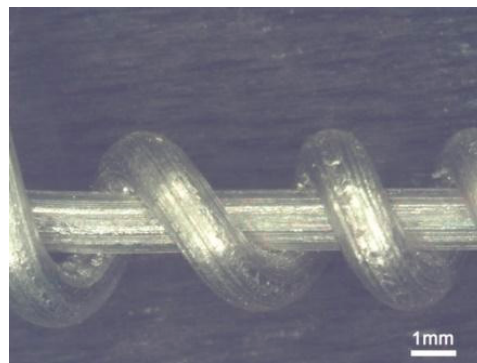


**Figure 7.** 0.50 wt.% MoB<sub>2</sub>.

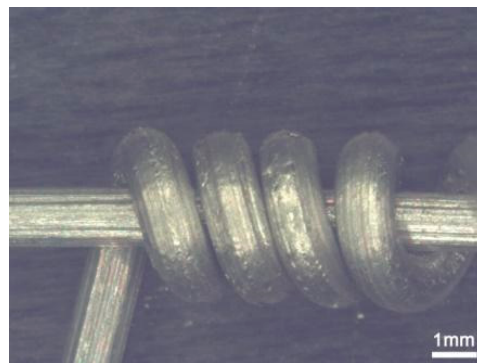


**Figure 8.** 0.75 wt.% MoB<sub>2</sub>.

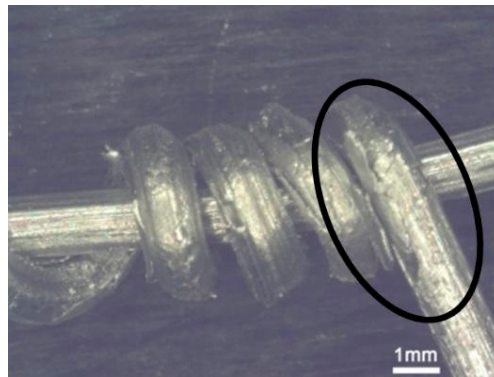


**Figure 9.** 1.00 wt.% MoB<sub>2</sub>.

### 3.4. Tensile Tests

The tensile test results presented in Figure 10 followed the ASTM B557-06 standard. The sample initial length was 250 mm with a  $6.6 \times 10^{-5}$  mm/mm/s strain rate. Clearly, the amount of diboride nanoparticles increased the ultimate tensile strength (UTS), likely following Orowan strengthening mechanisms. One can also observe that the UTS of the pure aluminum wires is 95 MPa, which is much higher than the strength reported in other research. i.e., 70 MPa [11]. This behavior can be explained with strengthening theory: With decreasing grain size (due to the cold forming), the mechanical strength increases [16].

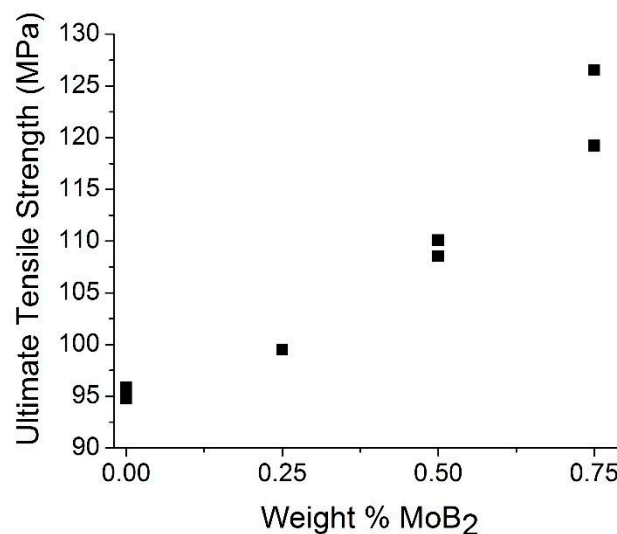


**Figure 10.** Measured ultimate tensile strength (UTS) as a function of the amount of MoB<sub>2</sub> in the wires.

### 3.5. Electrical Conductivity

Figure 11 presents the four-point probe measurements of the wires electrical conductivity at different temperatures. We first measured the voltage drop through the wires, while varying the amperage from 0.5 A to 10 A, in steps of 0.5 A. Since the sample geometry is known, we computed the conductivity of the samples. To measure the effect of temperature on the electrical conductivity, we submerged wires in ice water (0 °C) and then boiling water (100 °C). The response surface plot reveals how the MoB<sub>2</sub> nanoparticles lowered slightly the electrical conductivity of the wires. This effect is not entirely surprising as bulk MoB<sub>2</sub> possesses high electrical resistivity, i.e., 12.87  $\mu\Omega\cdot\text{cm}$  at 25 °C (13.4% IACS) [17]. Nonetheless, depending on the final application of the wires, such an increase in resistivity could not be detrimental.

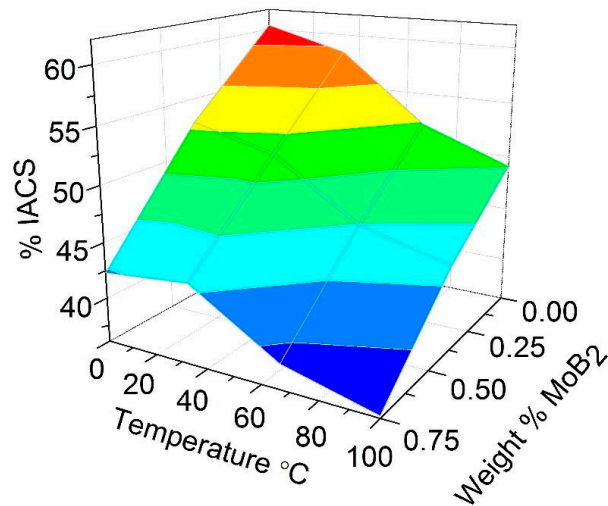


**Figure 11.** Measured electrical conductivity of the wires as a function of temperature and amount of MoB<sub>2</sub>.

As observed in Figure 11, the wires containing MoB<sub>2</sub> nanoparticles bear lower electrical conductivity as a function of temperature and amount of MoB<sub>2</sub>. As expected, the electrical resistivity (i.e., the reciprocal of conductivity) increases with temperature.

#### 4. Discussion

In order to provide additional tools for the prospective design of a filler, we supported our findings with pertinent descriptive statistics. The nomenclature used in the ensuing linear regression models is as follows:

% IACS = percent of International Annealed Copper Standard;

T = temperature in degrees Celsius;

UTS = ultimate tensile strength (MPa);

% MoB<sub>2</sub> = weight percent of molybdenum diboride.

The analysis of variance (ANOVA) obtained using Minitab™ is presented in Tables 1 and 2 for the fitted parameters and resulting *p*-values of the regression models, using a significance level ( $\alpha$ ) of 0.05. Equation (1) describes the ultimate tensile strength as a function of the amount of MoB<sub>2</sub> nanoparticles, yielding a very high coefficient of determination, i.e.,  $R^2 = 96.70\%$ . A similar trend was observed in Equation (2), describing the electrical conductivity as function of the percent of nanoparticles and temperature with  $R^2 = 93.69\%$ .

$$UTS = 95.24 + 9.36 \times \% MoB_2 + 36.76 \times (\% MoB_2)^2 \tag{1}$$

$$\% IACS = 58.42 - 12.83 \times T - 0.1412 \times \% MoB_2 \tag{2}$$

**Table 1.** Analysis of variance (ANOVA) of the model in Equation (1).

Source	DF	SS	MS	F	<i>p</i> -Value
Regression	2	839.65	419.82	58.90	0.001
Error	4	28.51	7.128		
Total	6	868.16			

**Table 2.** Analysis of variance (ANOVA) of the model in Equation (2).

Parameter	Coef	SE Coef	T-Value	p-Value
Constant	58.42	1.170	49.81	0.000
T	−12.83	2.160	−5.93	0.000
% MoB <sub>2</sub>	−0.141	0.014	−9.92	0.000

The ANOVA proves that for the UTS descriptive model (Equation (1)) the  $p$ -values are less than 0.05 which indicates that the content of MoB<sub>2</sub> is significantly affecting the wires strength. Similarly, in the linear regression model of the electrical conductivity (Equation (2)), the  $p$ -value, i.e.,  $p = 0.000$  proves that the % IACS is modified by the MoB<sub>2</sub> content. Along with the aforementioned high R<sup>2</sup> values, both models demonstrate how one can adjust the wire strength and conductivity by controlling the amount of MoB<sub>2</sub> nanoparticles added as nanocomposite pellets.

The quadratic form of Equation (1) may be related to a potential grain refining effect of the diborides on aluminum, i.e., by acting as potent catalytic substrates (heterogeneous nucleation sites) upon solidification. The effectiveness of diborides as nucleants was demonstrated in prior works [18]. The Hall-Petch equation indicates how yield strength is a function of the (grain size)<sup>−1/2</sup>. Therefore, in these wires, as the amount of diboride raises, the strength is heavily affected (a function of the square of the MoB<sub>2</sub> amount). The measurement of the wires' grain sizes as a function of MoB<sub>2</sub> is beyond the scope of this work but deserves an in-depth analysis in a follow-up research.

Nonetheless, this important improvement in mechanical strength for higher amounts of diboride nanoparticles is a significant discovery. In effect, if these wires are intended as fillers in tungsten inert gas (TIG) welding of aluminum parts, the addition MoB<sub>2</sub> nanoparticles can improve the strength of the welded joint without the need of additional alloying elements. The use of the MoB<sub>2</sub>-strengthened wires as fillers can be feasible if one considers the slight increase in electrical resistivity. Such higher resistivity can contribute to a higher temperature in the filler as the arc flows through it upon welding. Even a few degrees can be beneficial for faster and cleaner welds [19].

There is, however, a drawback brought about by the spooling test. The addition of the nanoparticles may interfere with the production of spools of these wires. This research uncovered that more than 1 wt.% MoB<sub>2</sub> nanoparticles could lead to wires with not enough ductility to be spooled. Yet, even smaller amounts can result in ductile wires with enough strength and adequate resistivity to be used as fillers in TIG welding of aluminum parts, this behavior can be verified with statistical analysis, i.e., the effects of the MoB<sub>2</sub> addition in the ultimate tensile strength and electrical conductivity.

## 5. Conclusions

Based on the results obtained we can affirm the following conclusions:

- The ultimate tensile strength of the wires can be controlled and raised by increasing the amount of MoB<sub>2</sub> nanoparticles added to the aluminum melt.
- According to the experimental results, higher amounts of MoB<sub>2</sub> nanoparticles present in the nanocomposite pellets leads to lower the electrical conductivity values.
- Wires coiling test revealed that smaller percentages than 1 wt.% MoB<sub>2</sub> result in sound wires able to be spooled as potential fillers for TIG welding of aluminum.
- The obtained results were corroborated via a multiple linear regression study of the ultimate mechanical strength and electrical conductivity as a function of the amount of nanoparticles added and temperature.

**Author Contributions:** D.F.-A. and O.M.S. Are the main contributors to the intellectual conception of the project. D.F.-A. and M.M.-G. manufactured the wires, analyzed and interpreted the data obtained from the characterization of those wires and wrote a significant portion of the manuscript. A.R.-M. prepared a significant portion of the manuscript.

**Funding:** This material is based upon work supported by the US National Science Foundation under Grants HRD 0833112 and 1345156 (CREST program).

**Acknowledgments:** The authors would like to thank the Materials Research Laboratory technician, Boris Rentería. The tensile test machine was acquired through a grant provided by the Solid Waste Management Authority of Puerto Rico.

**Conflicts of Interest:** The authors declare no conflict of interest.

## References

1. Li, L.; Zhang, K.; Qiu, J.; Wang, S.; Van, H.H.; Zhang, M. Solution assembly of vertically aligned diamond nanotube arrays from diamond nanocrystals. *Diam. Relat. Mater.* **2012**, *29*, 79–83. [[CrossRef](#)]
2. Tan, Z.; Li, Z.; Xiong, D.B.; Fan, G.; Ji, G.; Zhang, D. A predictive model for interfacial thermal conductance in surface metallized diamond aluminum matrix composites. *Mater. Des.* **2014**, *55*, 257–262. [[CrossRef](#)]
3. Lombardi, E.B.; Mainwood, A. A first principles study of lithium, sodium and aluminum in diamond. *Diam. Relat. Mater.* **2008**, *17*, 1349–1352. [[CrossRef](#)]
4. Chen, N.C.; Sun, F.H. Cutting performance of multilayer diamond coated silicon nitride inserts in machining aluminum-silicon alloy. *Trans. Nonferrous Met. Soc. China (Engl. Ed.)* **2013**, *23*, 1985–1992. [[CrossRef](#)]
5. Monachon, C.; Webe, L.R. Effect of diamond surface orientation on the thermal boundary conductance between diamond and aluminum. *Diam. Relat. Mater.* **2013**, *39*, 8–13. [[CrossRef](#)]
6. Yang, W.; Peng, K.; Zhou, L.; Zhu, J.; Li, D. Finite element simulation and experimental investigation on thermal conductivity of diamond/aluminium composites with imperfect interface. *Comput. Mater. Sci.* **2014**, *83*, 375–380. [[CrossRef](#)]
7. Feng, H.; Yu, J.K.; Tan, W. Microstructure and thermal properties of diamond/aluminum composites with TiC coating on diamond particles. *Mater. Chem. Phys.* **2010**, *124*, 851–855. [[CrossRef](#)]
8. Florián-Algarín, D.; Marrero, R.; Padilla, A.; Suárez, O.M. Strengthening of Al and Al-Mg alloy wires by melt inoculation with Al/MgB<sub>2</sub> nanocomposite. *J. Mech. Behav. Mater.* **2015**, *24*, 207–212. [[CrossRef](#)]
9. Florián-Algarín, D.; Padilla, A.; López, N.N.; Suárez, O.M. Fabrication of aluminum wires treated with nanocomposite pellets. *Sci. Eng. Compos. Mater.* **2014**, *22*, 485–490. [[CrossRef](#)]
10. Cullity, B.D.; Stock, S.R. *Elements of X-Ray Diffraction*, 3rd ed.; Prentice Hall: Upper Saddle River, NJ, USA, 2001; pp. 167–184.
11. *Standard Specification for Aluminum 1350—H19 Wire for Electrical Purposes 1*; ASTM B230/B230M; ASM International: Geauga County, OH, USA, 1975; pp. 1–4.
12. Suárez, O.M.; Stone, D.S.; Kailhofer, C.J. Measurement of electrical resistivity in metals and alloys using a commercial data acquisition software. *J. Mater. Educ.* **1999**, *20*, 341–356.
13. Stratton, S.W. *U.S. National Bureau of Standards Copper Wire Tattles*, 3rd ed.; Washington Government Printing Office: Washington, DC, USA, 1914.
14. Suárez, O.M.; Vazquez, J.; Reyes-Russi, L. Synthesis and characterization of mechanically alloyed Al/Al<sub>x</sub>Mg<sub>1-x</sub>B<sub>2</sub> composites. *Sci. Eng. Compos. Mater.* **2011**, *16*, 267–276. [[CrossRef](#)]
15. Malinovskis, P.; Palisaitis, J.; Persson, P.; Lewin, E.; Jansson, U. Synthesis and characterization of MoB<sub>2-x</sub> thin films grown by nonreactive DC magnetron sputtering. *J. Vac. Sci. Technol. A* **2016**, *34*, 031511. [[CrossRef](#)]
16. Howlader, M.K.; Marik, J.; Jandera, M. Cold-Forming effect on stainless steel sections. *Int. J. Steel Struct.* **2016**, *16*, 317–332. [[CrossRef](#)]
17. Shaw, A.H. *Physical Properties of Various Conductive Diborides and Their Binaries*. Ph.D. Thesis, Iowa State University, Ames, IA, USA, 2015.
18. Suárez, O.M. A study of the role of diborides in the heterogeneous nucleation of aluminum. *Rev. Met.* **2004**, *40*, 173–181.
19. De, A.; DebRoy, T. A smart model to estimate effective thermal conductivity and viscosity in the weld pool. *J. Appl. Phys.* **2004**, *95*, 5230–5240. [[CrossRef](#)]

